

Generating Digital Twins with Multiple Sclerosis Using Probabilistic Neural Networks

Jonathan R. Walsh,* Aaron M. Smith, Yannick Pouliot,
David Li-Bland, Anton Loukianov, and Charles K. Fisher
Unlearn.AI, Inc., San Francisco, CA

for the Multiple Sclerosis Outcome Assessments Consortium[†]

Abstract

Multiple Sclerosis (MS) is a neurodegenerative disorder characterized by a complex set of clinical assessments. We use an unsupervised machine learning model called a Conditional Restricted Boltzmann Machine (CRBM) to learn the relationships between covariates commonly used to characterize subjects and their disease progression in MS clinical trials. A CRBM is capable of generating digital twins, which are simulated subjects having the same baseline data as actual subjects. Digital twins allow for subject-level statistical analyses of disease progression. The CRBM is trained using data from 2395 subjects enrolled in the placebo arms of clinical trials across the three primary subtypes of MS. We discuss how CRBMs are trained and show that digital twins generated by the model are statistically indistinguishable from their actual subject counterparts along a number of measures.

* jon@unlearn.ai

[†] Data used in the preparation of this article were obtained from the Multiple Sclerosis Outcome Assessments Consortium (MSOAC). As such, the investigators within MSOAC contributed to the design and implementation of the MSOAC Placebo database and/or provided placebo data, but did not participate in the analysis of the data or the writing of this report.

I. INTRODUCTION

Statistical models that characterize and predict disease progression have the potential to become important tools for research and management of complex, chronic indications like Multiple Sclerosis (MS). In the context of clinical research, for example, statistical models of disease progression could be used to simulate different study designs [1], to identify patients who are likely to progress more rapidly than typical patients [2], or as external comparators in early stage clinical trials [3]. Despite the availability of Disease Modifying Therapeutics (DMTs) for MS, many clinical trials still compare experimental treatments to placebo controls [4–7], which can deter patients from enrolling in those trials. At the same time, the rich history of clinical trials in MS provides a high quality source of data about disease progression under placebo or non-DMT control conditions, creating an opportunity for statistical models to further the clinical understanding of MS and better inform the design and analysis of trials [8].

Ideally, a statistical model of disease progression would describe all of the clinical characteristics that are relevant for a patient with MS, how these characteristics change through time, their inter-relationships, and their variabilities. That is, in more technical terms, it would describe a joint probability distribution of the relevant clinical characteristics over time. Throughout, we refer to a sample drawn from this distribution as a *digital subject*. By definition, therefore, a digital subject is a computationally generated clinical trajectory with the same statistical properties as clinical trajectories from actual patients. The primary advantages of digital subjects, in comparison to data from actual patients, are that they present no risk of revealing private health information and make it possible to quickly simulate patient cohorts of any size and characteristics.

Although the ability to create digital subjects enables one to simulate cohorts of patients, there are many applications for which one would like to make predictions about a particular patient. A statistical model that is able to generate digital subjects can also be used for individual patients by generating digital subjects that have the same clinical characteristics as the patient of interest at a given date (such as the start of a clinical study). We refer to a digital subject that has been generated in order to match a particular patient as a *digital twin* of that patient, in analogy with the usage of the term “digital twin” in engineering applications [9]. For example, if the statistical model represents disease progression on a

placebo, then a digital twin provides a potential outcome – i.e., what would likely happen to this patient if she/he were given a placebo in a clinical trial? In more technical terms, a digital twin is a sample from a joint probability distribution of the relevant clinical characteristics at future times conditioned on the values of those characteristics at a previous time. We note that it is possible to generate multiple digital twins for any patient.

Evaluating the quality of a model that generates digital subjects or digital twins is more complex than the evaluation of traditional machine learning models. For example, it is necessary, but not sufficient, that the means, standard deviations, correlations, and auto-correlations of all covariates computed from cohorts of digital subjects agree with those computed from cohorts of actual subjects. Here, we introduce a concept called *statistical indistinguishability*. Digital subjects, or digital twins, are statistically indistinguishable from actual subjects if a statistical procedure designed to classify a given clinical record as a digital subject or an actual subject performs consistently with random guessing.

Creating a statistical model that can generate digital subjects and digital twins that are statistically indistinguishable from actual patients is no small feat, but recent advances in generative neural networks make it possible to train generative models for complex probability distributions [10–12], including time-dependent clinical data [2]. Here, we train a probabilistic generative neural network to create digital subjects with MS using a database of placebo arms aggregated across 7 historical clinical trials [8] covering many clinically relevant covariates including demographic information, relapses, the Expanded Disability Status Scale (EDSS) [13], and functional tests. To illustrate the concept of a digital subject for MS, Figure 1 shows two digital subjects generated by the model with the same starting characteristics (i.e., the two subjects are twins).

As a complex neurodegenerative disorder with a course that is “highly varied and unpredictable” [14], MS is both a good test-case for the application of machine learning methods as well as a disease area that would benefit from improved characterization and prediction of disease progression. Previous models for disease progression in MS include survival models [15–17], Markov models [18–20], and other methods [21–25]. Most of these studies aim to predict the progression of either the total EDSS score or relapses as they are common ways to characterize disease severity. To our knowledge, our approach is the first that models comprehensive subject-level clinical trajectories that go beyond the total EDSS score.

Multiple Sclerosis Digital Subject Example

Age (years): 44
 Sex: Female
 Race: White
 Region: Europe

MS type: RRMS
 Relapses in past year: 1
 Relapses in past 2 years: 2

Twin A

Time (months)	Baseline	3	6	9	12	15	18	21	24	27	30	33	36
Had Relapse	N	N	N	N	N	N	N	N	N	N	N	N	N
KFSS Pyramidal	2	2	3	2	2	2	3	3	3	3	2	2	2
KFSS Sensory	1	2	2	1	2	2	2	0	2	1	3	1	1
KFSS Bowel Bladder	1	1	2	1	2	2	1	2	1	1	2	2	1
KFSS Visual	1	0	1	1	1	0	1	1	1	1	3	3	3
KFSS Cerebellar	2	1	1	1	1	2	2	2	2	2	1	1	1
KFSS Brain Stem	1	0	1	1	1	2	2	2	2	1	1	1	1
KFSS Mental	0	0	0	0	0	0	0	0	1	0	1	2	2
Ambulation Score	0	0	0	0	0	0	0	0	0	0	0	1	0
EDSS Total Score	2.5	2.5	3.5	2	3	3.5	4	4	4	3.5	4	5	3.5
Timed 25-Foot Walk (s)	10.1	6.0	7.2	7.2	5.4	5.4	4.5	3.4	6.5	5.3	5.7	7.5	5.7
9-Hole Peg Test (Dominant Hand, s)	30.9	28.5	38.9	28.3	26.6	28.5	16.4	18.9	17.5	18.2	24.6	23.9	17.4
9-Hole Peg Test (Non-Dominant Hand, s)	43.3	30.7	39.1	26.5	22.7	22.7	26.8	28.5	32.0	19.7	18.3	23.4	21.7
PASAT, 3-second	50	58	59	59	55	59	51	57	57	59	60	59	59

Twin B

Time (months)	Baseline	3	6	9	12	15	18	21	24	27	30	33	36
Had Relapse	N	Y	N	N	Y	N	N	N	N	N	N	N	N
KFSS Pyramidal	2	2	2	2	3	3	2	3	4	4	4	4	4
KFSS Sensory	1	1	2	1	2	1	2	1	0	1	0	0	0
KFSS Bowel Bladder	1	1	1	0	1	0	1	0	0	0	0	0	0
KFSS Visual	1	1	1	1	2	1	0	0	0	0	0	0	0
KFSS Cerebellar	2	2	2	2	3	2	4	3	2	3	3	3	3
KFSS Brain Stem	1	2	1	2	3	2	2	2	1	1	1	0	1
KFSS Mental	0	2	2	2	1	1	0	0	0	0	0	0	0
Ambulation Score	0	0	0	0	2	3	1	2	1	3	4	3	3
EDSS Total Score	2.5	3	3	3	5.5	6	5	5.5	5	6	6.5	6	6
Timed 25-Foot Walk (s)	10.1	5.8	13.6	4.2	6.9	4.4	10.7	20.8	23.0	25.6	6.9	15.8	29.5
9-Hole Peg Test (Dominant Hand, s)	30.9	30.2	18.8	32.2	46.4	32.4	35.9	28.8	27.3	27.5	28.8	23.6	33.3
9-Hole Peg Test (Non-Dominant Hand, s)	43.3	41.9	32.8	26.2	36.9	29.7	24.7	20.3	31.4	22.3	24.9	27.0	41.4
PASAT, 3-second	50	46	32	55	48	57	50	59	47	52	37	24	40

FIG. 1. Example digital subjects for MS. Two digital subjects were sampled from the joint probability distribution learned by our model so that the two subjects share the same baseline characteristics (i.e., they are twins). Because the model is probabilistic, the two twins have different outcomes even though they share the same starting characteristics.

II. METHODS

A. Generating Digital Subjects with a Conditional Restricted Boltzmann Machine

Clinical data have many properties that make statistical modeling challenging. Data can come in varied modalities such as binary, ordinal, categorical, and continuous. Furthermore, observations may be occasionally or frequently missing. Conditional Restricted Boltzmann Machines (CRBMs) are well suited to address these challenges, and in past work we have found that CRBMs are able to effectively model disease progression in Alzheimer’s Disease [2].

A CRBM¹ is a class of probabilistic neural network that learns a joint probability distribution over time, and is closely related to Restricted Boltzmann Machines [26–30]. A CRBM learns the relationship between covariates at K visits expressed as a parametric probability distribution. For example, for $K = 3$ with a 3-month spacing between visits the distribution takes the form

$$p(\mathbf{x}(t+3), \mathbf{x}(t), \mathbf{x}(t-3)) = Z^{-1} \int d\mathbf{h} e^{-U(\mathbf{x}(t+3), \mathbf{x}(t), \mathbf{x}(t-3), \mathbf{h})}, \quad (1)$$

in which $\mathbf{x}(t)$ is the vector of covariates at time t (in months), \mathbf{h} is a vector of hidden variables, $U(\cdot)$ is called the energy function, and Z is a normalization constant. More details are provided in the Supporting Information.

The CRBM allows for approximate sampling from the joint probability distribution over all covariates and across K visits. Thinking of disease progression as a Markov process, the model can be used to probabilistically generate data for a subject at a visit given data from the previous $K - 1$ visits. For MS, we model data in 3-month intervals and find that modeling $K = 3$ simultaneous visits in the CRBM is sufficient to accurately generate long trajectories. In other words, we model MS clinical trajectories as a lag-2 Markov process.

The CRBM is used in an iterative fashion to generate clinical trajectories for digital subjects or digital twins. To generate a digital subject, the model is used to generate data at time zero (i.e., at baseline) by sampling from $p(\mathbf{x}(t = 0))$ using Markov Chain Monte Carlo (MCMC) methods. To generate a digital twin, the covariates at time zero (baseline) are set

¹ We use a version of CRBMs that have purely undirected connections, for which only a composite likelihood may be used for training, that is more appropriate for this application; see the Supporting Information for discussion.

equal to the observed covariates of a particular patient. Starting from these baseline data, the CRBM is used to generate data for the 3- and 6-month visits for that subject by sampling from $p(\mathbf{x}(t=6), \mathbf{x}(t=3)|\mathbf{x}(t=0))$. Then these sampled 3- and 6-month visit data may be used to generate data for the 9-month visit by sampling from $p(\mathbf{x}(t=9)|\mathbf{x}(t=6), \mathbf{x}(t=3))$. Similarly the sampled 6- and 9-month visit data may be used to generate data for the 12-month visit by sampling from $p(\mathbf{x}(t=12)|\mathbf{x}(t=9), \mathbf{x}(t=6))$. This continues as needed to create clinical trajectories of the desired length.

Under this framework, we can now define digital subjects and digital twins more formally. A digital subject is a clinical trajectory of length τ sampled from the joint distribution across all τ visits $\{\mathbf{x}(t)\}_{t=0}^{t=\tau} \sim p(\mathbf{x}(t=\tau), \dots, \mathbf{x}(t=0))$. A digital twin is a clinical trajectory of length τ in which the visits after $t=0$ are sampled from the conditional distribution $\{\mathbf{x}(t)\}_{t=3}^{t=\tau} \sim p(\mathbf{x}(t=\tau), \dots, \mathbf{x}(t=3)|\mathbf{x}(t=0))$.

One important concept is that digital subjects and digital twins are stochastic. Therefore, one can create many digital twins for a given patient. Each of these digital twins will have the same covariates at baseline, but their trajectories will differ after $t=0$. Taken together, these digital twins map out the distribution of possible clinical trajectories for that patient. Note that subjects in clinical trials do not receive different treatments at the baseline visit, so that digital twins may be created for subjects in any arm. If the CRBM models the progression of the disease under the control condition, then the model may be used to generate counterfactuals that can be used to estimate treatment effects. In this work, our training and validation data were collected entirely from placebo control arms of previously completed clinical trials so that digital subjects generated from the model are representative of placebo controls.

A schematic overview of our process for building the CRBM and generating digital twins is given in Figure 2.

B. Data

One legacy of the long history of clinical development for MS is a rich set of historical clinical trials with placebo arms. The Multiple Sclerosis Outcome Assessments Consortium (MSOAC) [8] has compiled data from 16 clinical trials that span three subtypes of MS: relapsing remitting (RRMS), secondary progressive (SPMS), and primary progressive (PPMS).

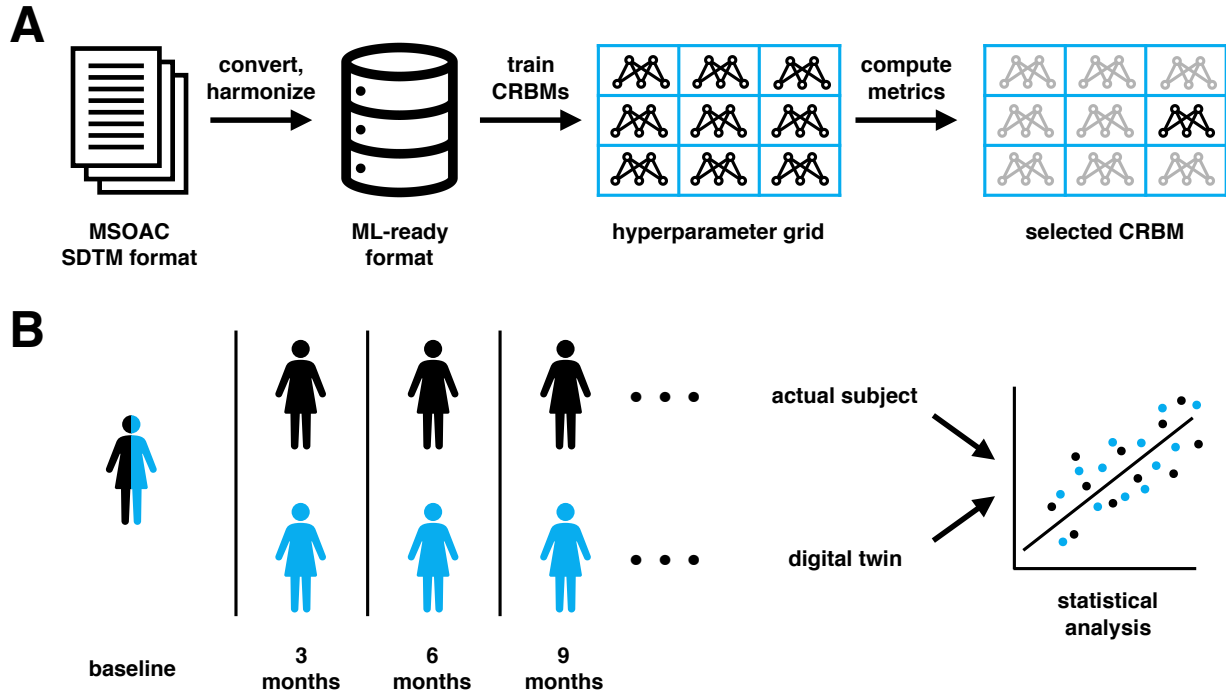


FIG. 2. **Overview.** A graphical summary of the process used to build the CRBM studied in this paper (A), and how digital twins are analyzed (B). To build the model, MSOAC data in SDTM format are converted to a numerical form suitable for machine learning. A set of models are trained that sweep over a grid of hyperparameters, variations in the way the model is trained. The final model is selected by computing metrics on validation data and choosing the best ranked model. An important feature of the CRBM is that it can create digital subjects and digital twins. Digital subjects are synthetic clinical records generated from the model. Digital twins are digital subjects whose baseline data is that of a given subject, allowing for subject-level predictions of outcomes. The CRBM is probabilistic, meaning many digital twins may be created for an actual subject and used to build distributions of predicted outcomes. In this work we use digital twins to analyze the quality of the CRBM as a disease progression model.

A database of placebo arms from 8 of these trials comprising 2465 subjects has been made available to qualified researchers. This database contains measurements spanning a number of domains including background information, questionnaires and functional assessments, medical history, and concomitant medications. No imaging or biomarker data is available.

MSOAC data are encoded according to the Study Data Tabulation Model (SDTM) format, a highly structured format commonly used to submit the results of clinical trials to regulatory authorities [31, 32]. Starting from the MSOAC placebo dataset, we standard-

Name	Category	Type	Longitudinal	Statistics	Missing [%]
Baseline Age	Background	Continuous	No	42 (10) [years]	1
Sex	Background	Binary	No	67% female	0
Race	Background	Binary	No	91% white	33
Region	Background	Categorical	No	64% Europe	58
MS type	Clinical	Categorical	No	65% RRMS	0
# of relapses, 1 year before baseline	Clinical	Ordinal	No	1.4 (0.8)	26
# of relapses, 2 years before baseline	Clinical	Ordinal	No	2.2 (1.3)	68
Relapse events	Clinical	Binary	Yes	95% no-relapse	0
KFSS bowel and bladder system	Clinical	Ordinal	Yes	0.83 (0.98)	13
KFSS brain stem system	Clinical	Ordinal	Yes	0.64 (0.87)	13
KFSS cerebellar system	Clinical	Ordinal	Yes	1.27 (1.17)	14
KFSS mental system	Clinical	Ordinal	Yes	0.58 (0.84)	13
KFSS pyramidal system	Clinical	Ordinal	Yes	1.86 (1.16)	13
KFSS sensory system	Clinical	Ordinal	Yes	1.19 (1.11)	13
KFSS visual system	Clinical	Ordinal	Yes	0.76 (1.00)	13
Ambulation EDSS component	Clinical	Ordinal	Yes	0.72 (1.36)	1
Timed 25-Foot Walk	Functional	Continuous	Yes	9.5 (14.6) [s]	1
Nine-Hole Peg, dominant hand	Functional	Continuous	Yes	24.8 (15.2) [s]	1
Nine-hole Peg, non-dominant hand	Functional	Continuous	Yes	27.7 (22.7) [s]	1
Paced Auditory Serial Addition Test (3s)	Functional	Continuous	Yes	47.4 (11.8)	1

TABLE I. Covariates used in the model are grouped into three categories: background, clinical, and functional. Background covariates are demographics that characterize the subject population. Functional covariates assess various aspects of MS-induced disability such as ambulation, motor skills, and cognitive function. Clinical covariates describe a subject’s clinical state such as the type of MS, degree of disability (through the Kurtzke Functional Systems Score, or KFSS, components), and relapse information. The Statistics column gives the mean and standard deviation of each covariate (or the dominant category for binary or categorical variables) at baseline in the combined training, validation, and test sets. The Missing column gives the percentage of missing data for each covariate at baseline.

ized and converted SDTM-formatted measurements into a tidy format [33] more suitable for statistical analysis and machine learning as described in the Supporting Information.

Twenty different covariates, described in Table I, were selected for inclusion in the model due to their clinical relevance and presence (non-missingness) in the dataset. They princi-

pally span background, clinical, and functional domains. Other clinically useful variables, such as questionnaires with data recorded for only a small fraction of subjects, were excluded. The components of EDSS and relapse events, the primary non-imaging endpoints in clinical trials, were included in the covariates modeled. Additionally, we added a simple longitudinal covariate that is modeled as binary, which is 1 at baseline and 0 otherwise. This allows the model to treat baseline as a special time.

Each selected covariate was classified as either longitudinal or static and as one of binary, ordinal, categorical, or continuous; these classifications affect how the covariate is modeled by the CRBM. The resulting dataset contains clinical trajectories for all subjects in the database in 3-month intervals for up to 48 months and an average duration of approximately 24 months.

Most subjects have a 3-month visit interval, but a 6-month interval is also present for approximately 800 subjects. Visit days were standardized to have a baseline visit day of 0, and longitudinal measurements were grouped into windows centered on each 90-day (3-month) visit and averaged. Any visit windows without a measurement for a particular covariate were recorded as missing.

We model each of the constituent components of the EDSS score, a combination of the 7-component Kurtzke Functional Systems Score (KFSS) assessment of function in a variety of body systems [13, 34, 35] and the ambulatory function of the subject. We discuss the advantages and methods around different approaches for representing these data more in the Supporting Information.

Before training, we removed 70 subjects that had essentially no data beyond baseline, resulting in a dataset with 2395 subjects. This dataset was divided into mutually exclusive training (50% of the data, or 1198 subjects), validation (20% of the data, or 479 subjects), and test (30% of the data, or 718 subjects) datasets. Due to the computational cost of associated with our training procedure, we had to rely on a single train-validation-test split, as opposed to a method like k-fold cross validation.

C. Training

A well-trained CRBM is able to generate digital subjects with the same statistical properties as actual subjects in the dataset. To accomplish this goal, we trained the CRBM via

stochastic gradient ascent to maximize a convex combination of a composite likelihood and an adversarial objective as previously described [2, 10]. The relative weight given to the likelihood and adversarial components of the objective function was treated as a hyperparameter.

Hyperparameters refer to various parameters of the model or training process that must be specified, but cannot be learned by applying gradient ascent to the objective function as with the main model parameters. These hyperparameters included the weighting of the likelihood and adversarial terms of the objective function, number of epochs, batch size, initial learning rate, number of hidden units, magnitude of parameter regularization, and sampling parameters (i.e., the number of Monte Carlo steps and the magnitude of temperature-driven sampling [10]). We performed a grid search over each of these dimensions in parallel, training a total of 1296 CRBMs with various hyperparameter choices to maximize an objective function on the training dataset.

After training the CRBMs in the grid search, we evaluated them using a variety of metrics that assess a model’s statistical performance as well as clinically important outcomes. All metrics were computed on the validation dataset. The statistical metrics are coefficients of determination (R^2 values) between the actual subjects from the test set and their digital twins for equal-time and lagged autocorrelations. Three clinical metrics were used, one measuring the ability to predict individual relapse events, another measuring the agreement between average EDSS progression values for the data and model, and the third measuring the agreement between chronic disease worsening (CDW) fractions for the data and model.

We adopted a minimax approach to choose a best performing model across the grid search. That is, we aimed to choose a CRBM that performed well across all metrics, even if it was not the best performing model on any single metric. To accomplish this, we ranked all N ($N=1296$) models from best (rank 1) to worst (rank N) for each metric and determined the worst rank across metrics for each model. We used this worst rank to choose the top 25% of models. This selected models that performed well on all metrics. To choose a best model from this set, we repeated the process on the clinical metrics alone, ranking models on the clinical metrics and determining the worst rank of each model. We selected the model with the lowest (best) worst rank and designated this as the “optimal” model. Narrowing the focus to the clinical metrics emphasized their importance in model selection.

The hyperparameters of this optimal model were then used to train a new, “final” model

on the combined training and validation datasets. All results that follow in the main text focus on the performance of this final model computed using the test dataset. More details on the hyperparameters, training procedures, and selection process for the optimal model are described in the Supporting Information.

III. RESULTS

A. Model Performance Across the Hyperparameter Sweep

The hyperparameter sweep trained 1296 models over a grid of hyperparameters on the training dataset. 83 of these models failed to finish training due to poor performance (e.g., due to too high of a learning rate), and were excluded from further evaluation because they were ranked lowest in model selection. We computed the model selection metrics using the validation dataset on the remaining 1213 models and determined the hyperparameters of the optimal model. These hyperparameters were used to train a new model on the combination of the training and validation datasets, which we refer to as “the final model”. For comparison, the test metrics were computed using both the optimal model determined from the validation set and the final model trained on combining training and validation sets.

The distributions of the validation metrics used for the hyperparameter sweep are shown in Figure 3, along with metric values for the optimal and final models. As expected, the optimal model performed well on all metrics without performing poorly on any individual metric. Furthermore, the performance of the optimal model was consistent across the validation and test datasets, with the largest the CDW fraction showing the largest difference. The performance of the optimal and final models on the test dataset were also quite similar, aside from the relapse prediction metric. This suggests that overall model performance is fairly stable with respect to changes to the dataset used for model training or evaluation.

B. Assessing Statistical Indistinguishability of Digital Twins

We say that digital twins and actual subjects are statistically indistinguishable if statistical analysis methods cannot differentiate the two groups better than random chance. Due

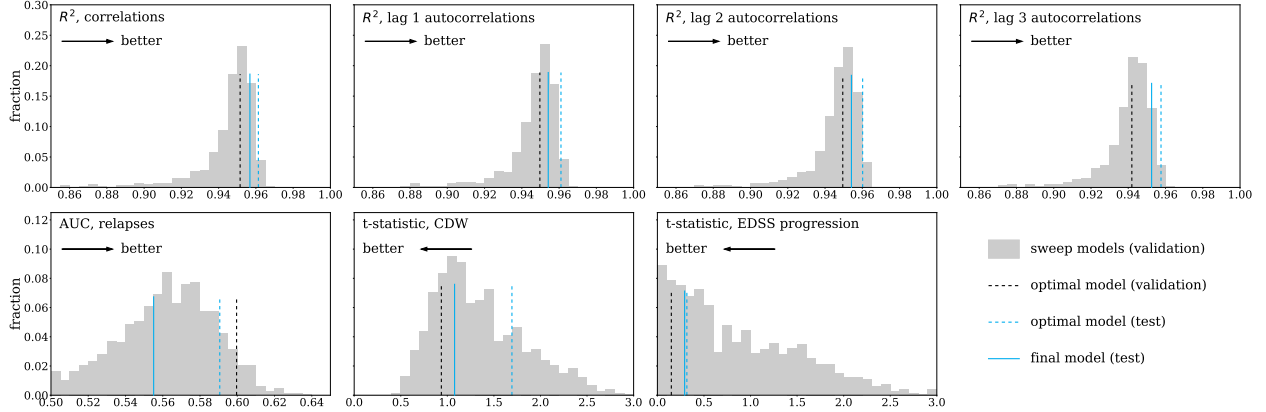


FIG. 3. **Metrics used to select hyperparameters for the best performing model.** For each metric used, the distribution of values across the hyperparameter sweep determined using the validation dataset is shown (gray histogram). The best performing model that was selected from this set is shown as a dashed black line at its value for each metric. The dashed blue line shows the value of the metric for this best performing model, computed on the test dataset. The solid blue line shows the value of the metric for the final model, computed on the test dataset. For each metric, an arrow indicates whether smaller or larger values are better.

to the complexity of clinical data, there are a number of ways to assess statistical indistinguishability. We focus on three different methods to quantitatively assess the degree of indistinguishability that span from subject- and covariate-level statistics to population-level statistics. The first compares the means, standard deviations, correlations, and autocorrelations of all covariates computed from the digital twins to those computed from the actual subjects, quantifying agreement using linear regression and coefficients of determination where appropriate. The second aims to quantify the agreement between the observed clinical trajectory of a particular patient and the distribution of potential clinical trajectories defined by his/her digital twins. The third trains logistic regression models to distinguish between actual subjects and their digital twins, quantifying performance with the area under the receiver operating characteristic curve (AUC).

To evaluate the statistical indistinguishability of digital twins, we created 1000 digital twins for each of the 718 actual subjects in the test dataset. The statistical properties of these twins were compared to the actual subjects in a number of ways to quantify the goodness-of-fit of the CRBM.

First, in Figure 4 we compare the means, standard deviations, correlations, and autocor-

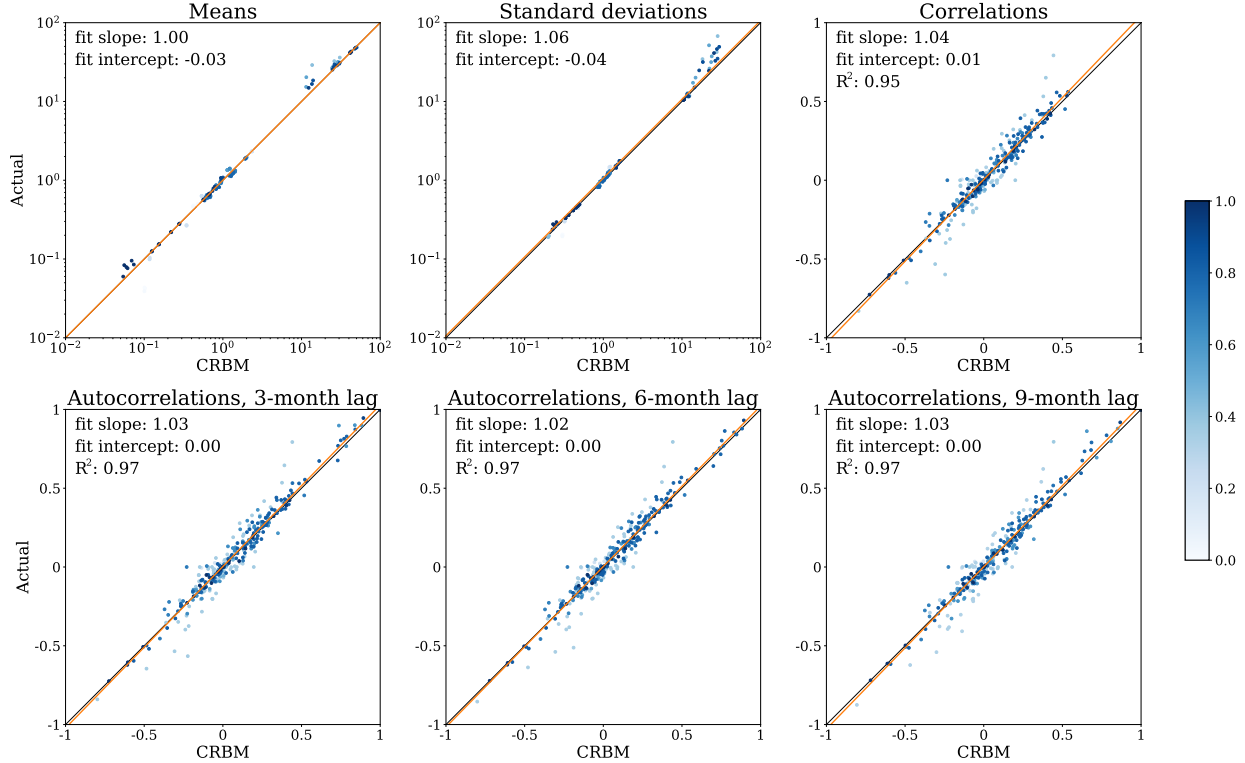


FIG. 4. **The model captures the leading statistical moments of the data.** Moments for the actual subject data are plotted against moments for digital twins for means, standard deviations, equal-time correlations, and lagged autocorrelations. Each digital twin contributes data for the same study duration as its actual subject counterpart up to 36 months. The means and standard deviations are compared at each visit, with a logarithmic scale used to accommodate differing scales of the covariates. For the equal-time and lagged autocorrelations the correlation coefficient is computed for each pair of covariates across all visits. In all cases the slope and intercept fit coefficients shown come from regressions weighted by the fraction of data present for each covariate. Points on the plot are darker if more data is present (see the color bar). These regressions estimate the relationship between actual subjects and digital twins. Theil-Sen regression is used for the means and standard deviations, which is outlier robust and appropriate for the widely varying scales present [36, 37]. For the equal-time and lagged autocorrelations, an ordinary least squares regression is used, which allows the R^2 values shown to be computed. The best fit line is shown for each comparison.

relations between covariates computed from the actual subjects and a cohort consisting of a single digital twin for each subject. The duration of the clinical trajectory of each digital twin was the same as the matched patient. We ignored the baseline time point when com-

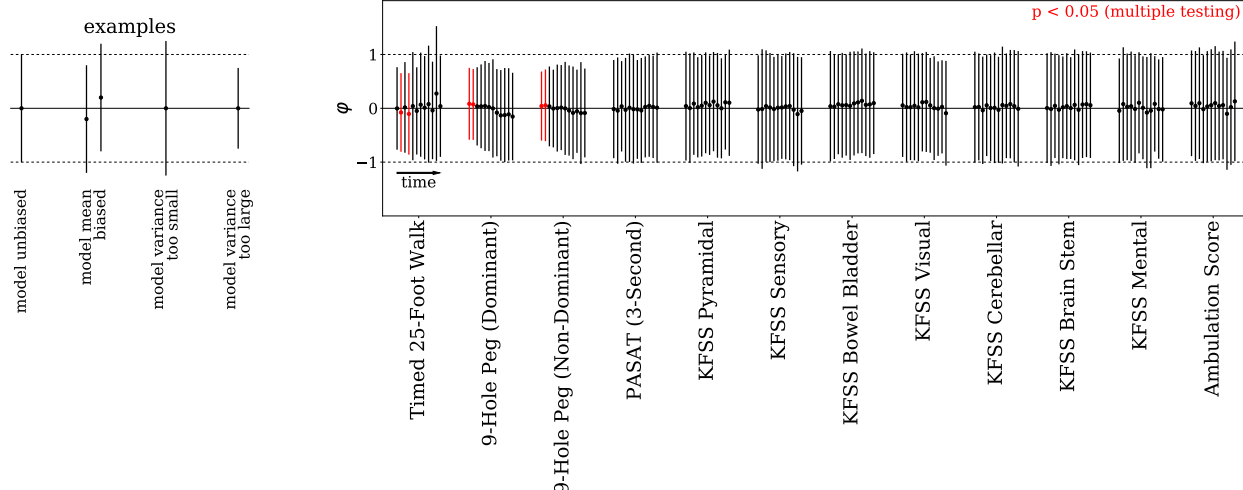


FIG. 5. **The model accurately simulates individual subject trajectories.** The mean and standard deviation of a statistic measuring subject-level agreement of the data with the CRBM, for each longitudinal covariate. Each visit beyond baseline is displayed using a point for the mean and an error bar for the standard deviation. The visits are ordered for each covariate, with data shown up to 36 months. For each subject, a p-value for each covariate at each visit is computed by comparing the data value to the distribution of values predicted by the CRBM under repeated simulations of digital twins for that subject. The inverse normal CDF is applied to this p-value to define a statistic, $\varphi \equiv \Phi^{-1}(p)$, and the mean and standard deviation of the distribution of φ over subjects are computed and plotted as a point and error bar. As the diagram on the left explains, if the CRBM is in statistical agreement with the data (unbiased) then the mean should be 0 and the standard deviation should be 1. Different types of bias are shown, and we label statistically significant cases ($p < 0.05$, with a confidence level adjusted to $0.05/144$ after applying a Bonferroni correction that factors in the 144 comparisons shown in the figure) in red.

putting the statistics because the actual subject and his/her digital twin have the same values of all covariates at the initial time point, by definition. All of the statistics computed from the cohort of digital twins agree with those computed from the cohort of actual subjects, with R^2 values for all comparisons greater than 0.95 and best fit coefficients close to their ideal values (i.e., 0 for the intercept, 1 for the slope).

Figure 4 compares a cohort of actual subjects to a cohort of matched digital twins based on population-level statistics. It is also important to quantify performance using statistics that are sensitive to subject-level agreement between an actual subject and his/her digital twins

as in Figure 5. We generated 1000 digital twins for each actual subject. For each subject, each covariate, and each visit, the samples from the digital twins form a distribution to which the observed data for the actual subject may be compared. We used the distribution defined by the digital twins to compute a tail area probability (i.e., p-value) for each observation, then used the inverse cumulative distribution function of the standard normal distribution to convert the p-value to a statistic, $\varphi = \Phi^{-1}(p)$, that has mean 0 and standard deviation 1 if the digital twins and subject data are drawn from identical distributions. This statistic controls for highly non-normal distributions of covariates better than a traditional z-score. We applied the Kolmogorov-Smirnov test to assess the if the distribution of these statistics is not $\mathcal{N}(0, 1)$ and mark any cases with statistically significant disagreement at $\alpha = 0.05$ after a Bonferroni correction.

Only early visits for the timed 25-foot walk and 9-hole peg test show statistically significant differences between actual subjects their digital twins, with the difference primarily due to the standard deviation of the φ distribution being too small. This indicates that the standard deviations of the distributions defined for these covariates by the digital twins are too large. These two functional tests are scored as time to completion of a task. Subjects can have large single-visit outliers in this time due to short-term ambulatory or motor difficulties, which is particularly challenging to learn. Although the model generally agrees with the data well, these results suggest that the CRBM generates large times for these tests too frequently.

Finally, in Figure 6, we demonstrate that a logistic regression model cannot distinguish between an actual subject and one of his/her digital twins better than random chance, which is a direct evaluation of statistical indistinguishability. For each time point (except baseline, when the actual subjects and their twins are the same by definition), we trained a logistic regression model to distinguish between each subject and his/her digital twins. In addition, we trained logistic regression models to distinguish between each subject and his/her digital twins using differences between time points. Over 36 months, nearly every logistic regression model’s performance is consistent with random guessing, meaning they are unable to distinguish between actual subjects and their digital twins better than random chance.

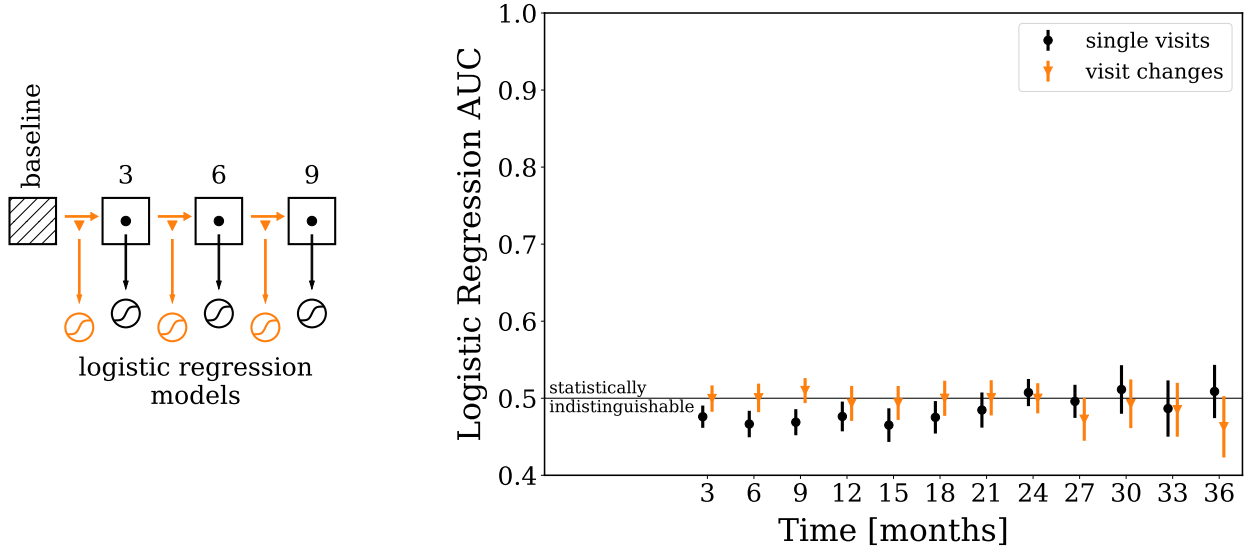


FIG. 6. **Digital twins are challenging to distinguish from actual subjects.** The area under the receiver operating characteristic curve (AUC) of logistic regression models trained to distinguish between actual data and their digital twins are shown. An AUC of 0.5 indicates the logistic regression model cannot differentiate between actual data and their digital twins better than random chance, while an AUC of 1 indicates the model can perfectly differentiate between the two groups. As the diagram at left shows, at each visit beyond baseline we evaluate the ability to distinguish digital twins from data either on data from a single visit (black circles) or the change in data from one visit to the next (orange triangles). In each case the point shown is the mean AUC is taken over 100 different simulations with different digital twins for each simulation; the error bars on the points show the standard deviation over simulations. The AUC for each simulation is estimated using 5-fold cross validation. Missing data from actual subjects is mean imputed; the corresponding values for the digital twins are assigned the same mean values to avoid biasing the logistic regression models.

IV. DISCUSSION

This work introduced three terms: *digital subjects*, *digital twins*, and the concept that digital subjects may be *statistically indistinguishable* from actual subjects. Using a dataset of subjects enrolled in the placebo arms of MS clinical trials, we trained a Conditional Restricted Boltzmann Machine to generate digital subjects. This dataset included demographic information and disease history, functional assessments, and components of the EDSS score. The model learned the relationship between covariates across multiple visits, treating dis-

ease progression as a Markov process; this means that given data for a subject at some number of prior visits, the model is capable of generating clinical trajectories representing the distribution of potential outcomes at future visits for that subject. Using a variety of statistical tests, we demonstrated digital subjects generated by the CRBM are statistically indistinguishable from actual subjects enrolled in the placebo arms of clinical trials for MS.

Modeling MS disease progression is challenging due to the complexity of endpoint measures and the varied course of the disease. Relapses are difficult to predict, and the EDSS score has multiple domains and depends on many components. It's likely that significant improvements could be made to our model by incorporating additional data on imaging-related endpoints is important as these endpoints are commonly studied in clinical trials, laboratory tests, and adverse events. Incorporating these additional covariates would enable generation of digital subjects with most of the covariates that are typically measured in MS clinical trials. In addition, incorporating data from subjects treated with interferons or other commonly-used DMTs would make it possible to generate cohorts of digital subjects representing broader control populations.

The ability to generate digital twins that are statistically indistinguishable from actual subjects enrolled in control arms of clinical trials is a powerful tool to understand disease progression and model clinical trials. Each digital twin represents a potential outcome of their matched patient; that is, what would likely happen to this patient if she/he were to receive a placebo in the context of a clinical trial? Models of potential outcomes are important tools for estimating treatment effects [38–40], and ability to generate digital twins representing per-subject controls opens the door to a variety of novel clinical trial analyses aimed at assessing responses to treatments for individual patients.

Taken in-context with previous work by the authors applying CRBMs to generate digital subjects for Alzheimer's Disease [2], this work suggests that approaches based on probabilistic neural networks like CRBMs will be broadly applicable to generating digital subjects across multiple diseases.

[1] N. Holford, S. Ma, and B. Ploeger, *Clinical Pharmacology & Therapeutics* **88**, 166 (2010).

[2] C. K. Fisher, A. M. Smith, and J. R. Walsh, *Scientific Reports* **9**, 1 (2019).

- [3] G. Carrigan, S. Whipple, W. B. Capra, M. D. Taylor, J. S. Brown, M. Lu, B. Arnieri, R. Coping, and K. J. Rothman, *Clinical Pharmacology & Therapeutics* **107**, 369 (2020).
- [4] F. D. Lublin, S. C. Reingold, and National Multiple Sclerosis Society (USA) Task Force on Placebo-Controlled Clinical Trials in MS, *Annals of neurology* **49**, 677 (2001).
- [5] C. H. Polman, S. Reingold, F. Barkhof, P. Calabresi, M. Clanet, J. Cohen, G. Cutter, M. Freedman, L. Kappos, F. Lublin, *et al.*, *Neurology* **70**, 1134 (2008).
- [6] B. M. Uitdehaag, F. Barkhof, P. K. Coyle, J. D. Gardner, D. R. Jeffery, and D. D. Mikol, *Current medical research and opinion* **27**, 1529 (2011).
- [7] Y. Zhang, A. Salter, E. Wallström, G. Cutter, and O. Stüve, *Therapeutic Advances in Neurological Disorders* **12** (2019).
- [8] N. G. LaRocca, L. D. Hudson, R. Rudick, D. Amtmann, L. Balcer, R. Benedict, R. Bermel, I. Chang, N. D. Chiaravalloti, P. Chin, J. A. Cohen, G. R. Cutter, M. D. Davis, J. DeLuca, P. Feys, G. Francis, M. D. Goldman, E. Hartley, R. Kapoor, F. Lublin, G. Lundstrom, P. M. Matthews, N. Mayo, R. Meibach, D. M. Miller, R. W. Motl, E. M. Mowry, R. Naismith, J. Neville, J. Panagoulas, M. Panzara, G. Phillips, A. Robbins, M. F. Sidovar, K. E. Smith, B. Sperling, B. M. Uitdehaag, J. Weaver, and Multiple Sclerosis Outcome Assessments Consortium (MSOAC), *Multiple Sclerosis (Houndmills, Basingstoke, England)* **24**, 1469 (2018).
- [9] M. Grieves and J. Vickers, in *Transdisciplinary Perspectives on Complex Systems: New Findings and Approaches*, edited by F.-J. Kahlen, S. Flumerfelt, and A. Alves (Springer, 2016).
- [10] C. K. Fisher, A. M. Smith, and J. R. Walsh, arXiv:1804.08682 [cs, stat] (2018).
- [11] G. W. Taylor and G. E. Hinton, in *Proceedings of the 26th Annual International Conference on Machine Learning, ICML '09* (ACM, New York, NY, USA, 2009) pp. 1025–1032, event-place: Montreal, Quebec, Canada.
- [12] G. W. Taylor, G. E. Hinton, and S. T. Roweis, in *Advances in Neural Information Processing Systems 19*, edited by B. Schölkopf, J. C. Platt, and T. Hoffman (MIT Press, 2007) pp. 1345–1352.
- [13] J. F. Kurtzke, *Neurology* **33**, 1444 (1983).
- [14] M. M. Goldenberg, *Pharmacy and Therapeutics* **37**, 175 (2012).
- [15] A. Scalfari, A. Neuhaus, M. Daumer, G. C. Ebers, and P. A. Muraro, *Neurology* **77**, 1246 (2011).
- [16] H. Tremlett, Y. Zhao, P. Rieckmann, and M. Hutchinson, *Neurology* **74**, 2004 (2010).

- [17] S. Vukusic and C. Confavreux, *Current Opinion in Neurology* **20**, 269 (2007).
- [18] S. A. Gauthier, M. Mandel, C. R. G. Guttmann, B. I. Glanz, S. J. Khoury, R. A. Betensky, and H. L. Weiner, *Neurology* **68**, 2059 (2007).
- [19] J. Palace, T. Bregenzer, H. Tremlett, J. Oger, F. Zhu, F. Zhu, M. Boggild, M. Duddy, and C. Dobson, *BMJ open* **4**, e004073 (2014).
- [20] Y. Hou, Y. Jia, and J. Hou, *Scientific Reports* **8** (2018).
- [21] F. Pellegrini, M. Copetti, M. P. Sormani, F. Bovis, C. de Moor, T. P. Debray, and B. C. Kieseier, *Multiple Sclerosis (Houndmills, Basingstoke, England)* (2019).
- [22] M. T. Law, A. L. Traboulsee, D. K. Li, R. L. Carruthers, M. S. Freedman, S. H. Kolind, and R. Tam, *Multiple Sclerosis Journal - Experimental, Translational and Clinical* **5** (2019).
- [23] M. Lawton, K. Tilling, N. Robertson, H. Tremlett, F. Zhu, K. Harding, J. Oger, and Y. Ben-Shlomo, *Journal of Clinical Epidemiology* **68**, 1355 (2015).
- [24] A. Achiron, Y. Barak, and Z. Rotstein, *Multiple Sclerosis (Houndmills, Basingstoke, England)* **9**, 486 (2003).
- [25] A. Achiron, *Journal of Neurology* **251 Suppl 5**, v65 (2004).
- [26] D. H. Ackley, G. E. Hinton, and T. J. Sejnowski, *Cognitive science* **9**, 147 (1985).
- [27] G. E. Hinton and R. R. Salakhutdinov, *Science* **313**, 504 (2006).
- [28] R. Salakhutdinov and G. Hinton, in *Artificial Intelligence and Statistics* (2009) pp. 448–455.
- [29] G. Hinton, *Momentum* **9**, 926 (2010).
- [30] I. Goodfellow, J. Pouget-Abadie, M. Mirza, B. Xu, D. Warde-Farley, S. Ozair, A. Courville, and Y. Bengio, in *Advances in neural information processing systems* (2014) pp. 2672–2680.
- [31] W. R. Kubick, S. Ruberg, and E. Helton, *Drug Information Journal* (2016).
- [32] L. D. Hudson, R. D. Kush, E. Navarro Almario, N. Seigneuret, T. Jackson, B. Jauregui, D. Jordan, R. Fitzmartin, F. L. Zhou, J. K. Malone, J. Galvez, and L. B. Becnel, *Clinical and Translational Science* **11**, 342 (2018).
- [33] H. Wickham *et al.*, *Journal of Statistical Software* **59**, 1 (2014).
- [34] J. F. Kurtzke, *Neurology* **11**, 686 (1961).
- [35] J. F. Kurtzke, *Neurology* **15**, 654 (1965).
- [36] H. Theil, *Nederl. Akad. Wetensch., Proc.* **53**, 386 (1950).
- [37] P. K. Sen, *Journal of the American Statistical Association* **63**, 1379 (1968).
- [38] D. B. Rubin, *Scandinavian Journal of Statistics* **31**, 161 (2004).

- [39] G. W. Imbens and D. B. Rubin, in *Microeconometrics* (Springer, 2010) pp. 229–241.
- [40] S. R. Künzel, J. S. Sekhon, P. J. Bickel, and B. Yu, Proceedings of the national academy of sciences **116**, 4156 (2019).
- [41] V. Mnih, H. Larochelle, and G. E. Hinton, arXiv preprint arXiv:1202.3748 (2012).
- [42] J. Tubiana and R. Monasson, Physical Review Letters **118**, 138301 (2017).
- [43] C. Gouriéroux and J. Jasiak, Journal of Forecasting **25**, 129 (2006).
- [44] G. Desjardins, A. Courville, Y. Bengio, P. Vincent, and O. Delalleau, in *Proceedings of the Thirteenth International Conference on Artificial Intelligence and Statistics* (MIT Press Cambridge, MA, 2010) pp. 145–152.
- [45] G. Desjardins, A. Courville, Y. Bengio, P. Vincent, and O. Delalleau, in *Proceedings of the Thirteenth International Conference on Artificial Intelligence and Statistics* (2010) pp. 145–152.

Appendix A: Data Processing and Datasets

Data from the MSOAC database is stored in Study Data Tabulation Model (SDTM) format. The transformation of data from SDTM format to a format useful for statistical analysis and machine learning requires many steps. The MSOAC database, which aggregates data from multiple clinical trials in SDTM format, is a clean and high-quality data source. Because source data in the MSOAC database are from different clinical trials, particular attention must be paid to harmonization, to ensure that data for the same concept are represented the same way. This can easily happen, for example, if different trials use different conventions to encode measurements.

Besides harmonization, data must be converted from SDTM format to a data format that is suitable for analysis. SDTM represents observations in terms of variables encoding broad contextual data about the observation, while statistical analyses use tabular formats where covariates come with implicit definitions and values for covariates are plain data types. This tabular format is well described by the tidy data concept [33].

To carry out data processing, we have built a software library in `python` that makes it easier to harmonize data, convert between formats, and document and test the steps taken. This toolkit is described in [2], and has proven effective here.

1. Covariates Used in Training

111 covariates were extracted from the MSOAC database using the processing methods described above, from which we selected a subset of 20 covariates relevant to modeling MS progression that are without substantially missing data or are relevant for clinical trials. We note that many covariates not included in the model describe components of questionnaires rarely measured (43 covariates from SF-12, BDI-II, and RAND-36), characterization of disability in medical history (20 covariates), or medication data that lacked dosing time information (16 covariates).

Although subjects were part of placebo control arms, they may have been taking medications that are part of the standard of care for treating MS or other conditions. Some of these medications, such as those considered to be disease modifying, are known to influence the evolution or presentation of MS. DMT medications were rarely used (5% of subjects

received them) and were likely provided as rescue therapies from relapses or adverse events. However, as dosing time information was not provided, these variables were not included in dataset.

The processing of components of the EDSS score merit discussion. The EDSS score is especially challenging to model. The lower range of EDSS is defined by a complex scoring function applied to the components of the Kurtzke Functional Systems Score (KFSS) components, a 7-component test assessing function in variety of bodily systems [13, 34, 35]. The upper range of EDSS is principally defined by the subject’s ability to walk. Due to the nature of scoring, some values are much more likely than others, giving a very multi-modal marginal distribution of EDSS scores. We chose to model the individual KFSS components and ambulatory impairment of subjects rather than model the total score directly, allowing the model to learn the simpler constitutive covariates and the relationships between them.

Unfortunately, the MSOAC database does not record the ambulatory impairment component of EDSS directly. Instead, we infer this *ambulation score* from the EDSS score and encode it as an ordinal covariate. The covariate is determined by the number of 0.5-units the reported EDSS score is above the ambulation cutoff (4.5); cases where the EDSS score is equal to or smaller than the ambulation cutoff yield an ambulation score of 0. Note that we are assuming that subjects with high KFSS scores have impaired ambulatory function. KFSS scoring rubrics do not provide consistent guidelines for assigning scores above the ambulation cutoff, indicating this assumption is valid.

As a cross-check, we are able to compute the EDSS score from the KFSS components alone. When the EDSS score was outside of the ambulatory range, we were able to compare the reported EDSS score with the value given by the KFSS components. In approximately 10% of cases we found a disagreement, and in a majority of these cases we were able to clearly identify an apparent mis-scoring of EDSS based on the reported KFSS component scores.

When training the CRBM, performance is improved the scale of each covariate is similar. Therefore, we apply a normalizing transformation to most covariates to ensure the range of each covariate is of order 1. For binary and categorical covariates no normalization is applied, while for ordinal covariates we scale the covariate by its maximum so that the values range between 0 and 1. For continuous covariates we apply different normalizing transformations depending on the features of the covariate. In Table II we give these transformations along

Name	Encoding	Domain	Normalizing Transformation
Baseline Age	Continuous	18 – 72	Standardization
Sex	Binary	{0, 1}	None
Race	Binary	{0, 1}	None
Region	1-hot, 3 labels	{0, 1}	None
Baseline	Binary	{0, 1}	None
MS type	1-hot, 3 labels	{0, 1}	None
# of relapses, 1 year before baseline	Ordinal	{0, 1, ..., 7}	Scaled by 1/7
# of relapses, 2 years before baseline	Ordinal	{0, 1, ..., 14}	Scaled by 1/14
Relapse events	Binary	{0, 1}	None
KFSS bowel and bladder system	Ordinal	{0, 1, ..., 6}	Scaled by 1/6
KFSS brain stem system	Ordinal	{0, 1, ..., 5}	Scaled by 1/5
KFSS cerebellar system	Ordinal	{0, 1, ..., 5}	Scaled by 1/5
KFSS mental system	Ordinal	{0, 1, ..., 5}	Scaled by 1/5
KFSS pyramidal system	Ordinal	{0, 1, ..., 6}	Scaled by 1/6
KFSS sensory system	Ordinal	{0, 1, ..., 6}	Scaled by 1/6
KFSS visual system	Ordinal	{0, 1, ..., 6}	Scaled by 1/6
Ambulation component of EDSS score	Ordinal	{0, 1, ..., 11}	Scaled by 1/11
Timed 25-Foot Walk	Continuous	2 – 300	Logit scaled to range
Nine-Hole Peg, dominant hand	Continuous	10 – 260	Logit scaled to range
Nine-hole Peg, non-dominant hand	Continuous	10 – 260	Logit scaled to range
Paced Auditory Serial Addition Test	Continuous	0 – 60	Logit scaled to range

TABLE II. Covariates used in the model, their domain, encoding, and the normalizing transformation applied to them. Categorical covariates (which are 1-hot encoded) and binary covariates have no normalizing transformation, while ordinal covariates are scaled to have a maximum value of 1. Continuous variables are normalized in different ways, but each results in a range where values are not much larger than 1.

with the encoding and its natural range.

For age, the “standardization” transform means we subtract the mean and divide by the standard deviation, where both moments are determined from the training set. The functional assessment covariates (timed 25-foot walk, 9-hole peg test, and paced auditory serial addition test (PASAT)) all use a logit transformation. The functional form of these

transformations is

$$\tilde{x} = \log \left(\frac{x - (x_- + \delta)}{(x_+ + \delta) - x} \right), \quad (\text{A1})$$

where x_{\pm} are upper and lower limits of the covariate (the range values given in the table) and δ is a buffer to prevent the argument from being too small or large (we use $\delta = 0.5$). This transformation, like the others used, are invertible, meaning we can transform from the representation of the data generated by the CRBM to retrieve the natural representation of the data. For the PASAT test, we choose to model the covariate as continuous (rounding the value when using the model output) rather than ordinal due to the large number of possible values.

Appendix B: CRBMs

1. Summary of CRBMs

Restricted Boltzmann machines (RBMs) [26, 29] are a well-known class of probabilistic neural networks capable of representing the complex interrelationships between variables in large datasets. They provide several features critical to modeling clinical data (see the supplementary material in [2]).

A Conditional Restricted Boltzmann Machine (CRBM) is a type of probabilistic model that provides a way to model time series data by leveraging the natural capabilities of Boltzmann machines. In fact a CRBM is an RBM in which the organization of the visible units is particular to the time-dependence of the data. That is, without particular temporal labels on the visible units of the CRBM, the model is simply an RBM. These models can be trained the same way as RBMs, except that the temporal nature of the data potentially requires a reorganization of the training data.

In the original development [12, 41], CRBMs are defined as a particular kind of graphical model encompassing an RBM whose probability distribution depends conditionally on previous time points.

That is,

$$p(\mathbf{x}_{t+k} | \mathbf{x}_{t+k-1}, \dots, \mathbf{x}_t) = Z^{-1} \int d\mathbf{h} e^{-U(\mathbf{x}_{t+k}, \mathbf{h} | \mathbf{x}_{t+k-1}, \dots, \mathbf{x}_{t+1}, \mathbf{x}_t)}, \quad (\text{B1})$$

in which \mathbf{x}_t is the vector of covariates at time index t , \mathbf{h} is a vector of hidden variables, Z is a normalization constant, and $U(\cdot | \cdot)$ is the conditional energy function. Here the conditional

energy function is a family of functions parametrized by linear functions of the previous time points. Graphically, this is a graphical model in which there are directed arrows extending from the previous time points to the hidden units of an RBM.

In our incarnation we have generalized the definition slightly in two regards. First, we allow some sector of the visible variables to be time-independent (denoted $\mathbf{x}_{\text{static}}$). Secondly we modify the model graph so that it admits exclusively *undirected* arrows. We can recover the original notion of a CRBM by simply conditioning on the prior time points' visible units.

Specifically, the joint probability distribution of $k + 1$ time-adjacent vectors

$$p(\mathbf{x}_{t+k}, \dots, \mathbf{x}_{t+1}, \mathbf{x}_t, \mathbf{x}_{\text{static}}) = Z^{-1} \int d\mathbf{h} e^{-U(\mathbf{x}_{t+k}, \dots, \mathbf{x}_{t+1}, \mathbf{x}_t, \mathbf{x}_{\text{static}}, \mathbf{h})}, \quad (\text{B2})$$

in which the energy function $U(\cdot)$ takes the form,

$$U(\mathbf{x}_{t+k}, \dots, \mathbf{x}_{t+1}, \mathbf{x}_t, \mathbf{x}_{\text{static}}, \mathbf{h}) = \sum_{i=0,1,\dots,k,\text{static}} \left[\sum_j a_{i,j}(\mathbf{x}_{t+i,j}) + \sum_{j\mu} W_{i,j\mu} \frac{\mathbf{x}_{t+i,j} h_\mu}{\sigma_{i,j}^2 \epsilon_\mu^2} \right] + \sum_\mu b_\mu(h_\mu). \quad (\text{B3})$$

Each unit of the visible and hidden layers has bias parameters determined by the choice of functions $a_{ij}(\cdot)$ and $b_\mu(\cdot)$, as well as scale parameters σ_{ij} and ϵ_μ . The connection between the layers is parameterized by the weight matrices $W_{i,j\nu}$.

Understood as a single RBM, our CRBM contains the visible units for multiple time points, with a standard hidden layer. The visible units are organized as:

$$\mathbf{x}_{\text{CRBM}} = \mathbf{x}_{t+k} \oplus \mathbf{x}_{t+k-1} \oplus \dots \oplus \mathbf{x}_t \oplus \mathbf{x}_{\text{static}}, \quad (\text{B4})$$

where k is the time lag of the model and \oplus signifies concatenation. The static units are only used once over all time points, as they are constant over all times. The model learns the complete joint probability distribution between all $k + 1$ adjacent time points simultaneously, $p(\mathbf{x}_{t+k}, \dots, \mathbf{x}_t, \mathbf{x}_{\text{static}})$. That means that *any* conditional sampling of the data may be performed, such as predicting the data for a time point given the previous k time points. A baseline cohort may be simulated by sampling from the model and using the first time point. This treatment of the data to allow for learning inter-dependence between time points is the only distinction of a CRBM over a standard RBM. In Figure 7, we show a schematic diagram highlighting the differences between an RBM, the CRBM we describe here, and the CRBM originally described in [12, 41].

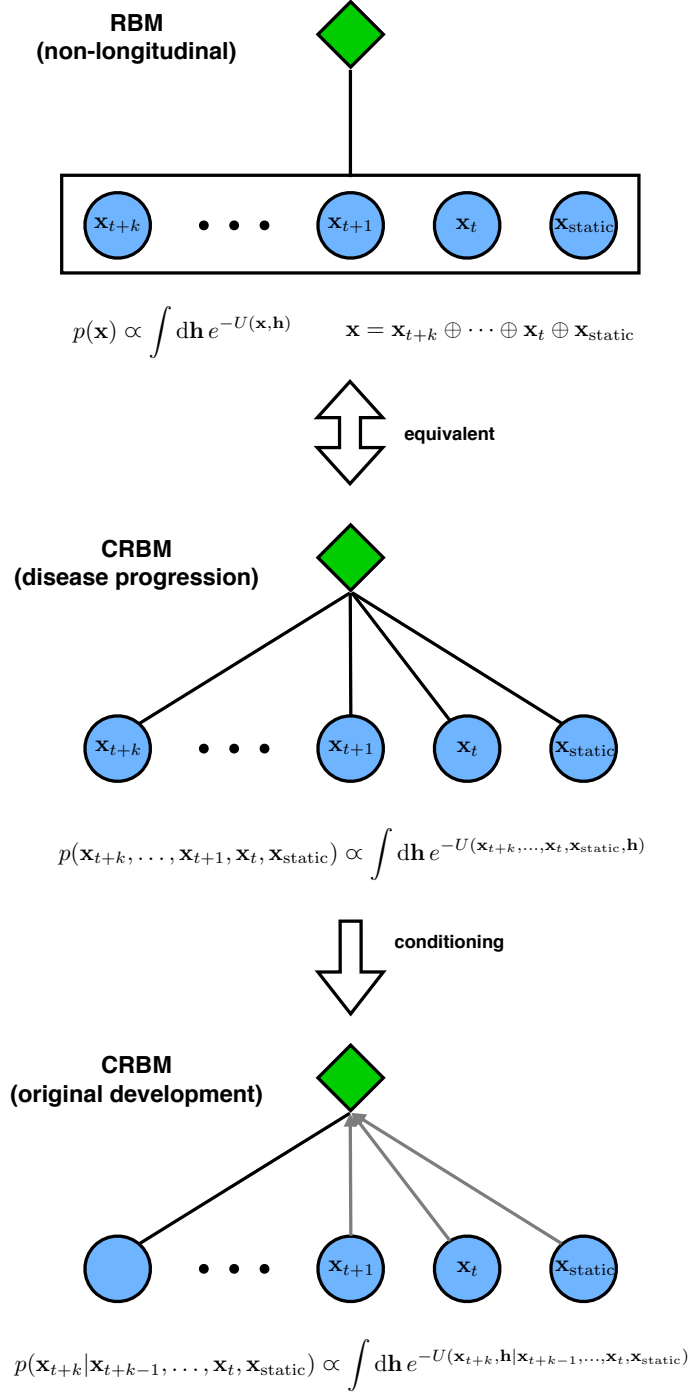


FIG. 7. **Architectures of RBMs and CRBMs.** A schematic architecture of the CRBM used in this work is shown in the middle, compared to an RBM, which is an equivalent architecture, and the original CRBMs, which are described in the text. Both the RBM and CRBM used here have completely undirected connections, while the original CRBM has directed connections except for the last time point. Directed connections are shown as gray arrows.

2. Training methods

The CRBM is trained on the data from adjacent triples of time points. If \mathbf{x}_t is the vector of time-dependent variables for a patient at time t (in months) and $\mathbf{x}_{\text{static}}$ is the vector of static variables for the same patient, then the visible units used to train the CRBM are $\mathbf{v} = \{\mathbf{x}_{t+6}, \mathbf{x}_{t+3}, \mathbf{x}_t, \mathbf{x}_{\text{static}}\}$, a concatenation of the data from the adjacent time points t , and $t + 3$ months, and $t + 6$ months with the static variables represented only once.

As discussed in the main text, to train the CRBM we divided the 2395 subjects in the dataset up into 3 parts: training (50% of subjects), validation (20% of subjects), and test (30% of subjects). Training was done in two stages. First we train a large number (1296) models over a grid of hyperparameters and measure the performance of models according to a number of metrics. The hyperparameters of the best-performing model were used to train a model on the combination of the training and validation data.

To train the model, we take data from a subject’s trajectory and transform it to the format used by the model. This involves 3 steps:

1. For each subject we create vectors of data from all possible sets of 3 consecutive visits. For example if a subject has data through 12 months we create vectors for 0, 3, and 6 months, 3, 6, and 9 months, and 6, 9, and 12 months. Repeated occurrences of the static (non-longitudinal) covariates are dropped so that they only appear once in the vector.
2. Frequently subjects may be missing data. If any vector has no longitudinal data for the last visit, it is removed. This removes certain vectors in cases where the subject has missed visits.
3. We standardize the data by transforming covariates so that their range is of order 1. These are the transformations discussed in Section A.

Note that because each subject typically has trajectories much longer than the 6-month time window (trajectories up to 57 months are used), the number of samples in the combined training and validation datasets (11129) is much larger than the number of subjects. When training, samples are all shuffled so that minibatches contain a mixture of subjects and times.

The CRBM has a single hidden layer of ReLU units [42], and is trained using stochastic gradient descent according to the setup of [10]. The objective \mathcal{C} is a linear combination of log-likelihood \mathcal{L} and adversarial \mathcal{A} objectives,

$$\mathcal{C} = -\gamma\mathcal{L} - (1 - \gamma)\mathcal{A}, \quad (\text{B5})$$

in which γ is a parameter weighing the relative size of the two objectives. Here we use a random forest classifier for the adversary. The parameter γ is one of the hyperparameters selected via a grid sweep.

It is important to note that the likelihood \mathcal{L} is the likelihood of observing a given three-timepoint trajectory according to the model’s distribution. It is not the likelihood of observing an arbitrary-length trajectory generated by the model via conditional sampling. In this regard the the model minizes a *partial likelihood* with respect to arbitrary length trajectories.

3. Temperature driven sampling

An important concept for stochastic models is the notion of mixing, which contributes to the ability of the model to simultaneously represent multiple different groups in the dataset. A model with poor mixing cannot, for example, represent multiple subtypes of MS well or effectively learn multiple modes of disease progression. To address this, we employ a simple approach to improve the mixing of the CRBM when generating digital subjects or digital twins. The underlying RBM that the CRBM is built upon can integrate the concept of temperature, which enters the joint probability distribution as $p(\mathbf{v}, \mathbf{h}) = Z^{-1}e^{-\beta E(\mathbf{v}, \mathbf{h})}$, where β is the inverse temperature and \mathbf{v} and \mathbf{h} are the visible and hidden units of the model. By drawing the inverse temperature from an autoregressive gamma process [43] with mean 1, a small standard deviation, and a non-zero autocorrelation, we can improve the rate of mixing [10]. When β is small, mixing is fast and different modalities can be explored and more efficiently learned. Setting the mean of β to 1 ensures that the samples stay close to the true distribution, and when sampling we anneal the standard deviation of β to 0 with no autocorrelation to ensure that the end of the Markov chain samples from the true distribution. While training, we do not anneal and use an autocorrelation close to 1 (0.9) to ensure that the inverse temperatures evolve slowly and the system can remain near equilibrium. Unlike parallel tempering [44, 45], this algorithm for *driven sampling* does not

sample from the exact distribution, and instead samples from a *similar* distribution to the RBM that has fatter tails. However, this approach adds only a small computation cost and appears to improve training outcomes (in this and other applications); see [10] for details.

Appendix C: Hyperparameter Sweep and Model Selection

1. Hyperparameters

Multiple hyperparameters are used in training the CRBM. To select an optimal model, we trained a set of models over a grid of these hyperparameters and chose the model that performed the best on a set of metrics computed on the validation dataset. The grid, along with the hyperparameters of the selected model are shown in Table III. The grid was chosen to scan over reasonable ranges of key hyperparameters and fix others at reasonable values that are not expected to significantly affect model performance. Note that the number of samples in the combination of the training and validation datasets (11129) and the number of visible units (53) are used in defining the hyperparameters for training the model. The number of hidden units is set as a fraction of the number of visible units, and the batch size is set as a fraction of the number of samples. In total, 1296 models were trained.

2. Selection Metrics

Because CRBMs are generative, model performance can be assessed in a number of ways. This makes it challenging to find an optimal model across the hyperparameter grid, as different models may be relatively better or worse given the evaluation method. We addressed this by selecting models that performed well across a number of metrics.

We chose metrics in two categories: ones that assessed the statistical quality of samples generated by the model, and ones that assessed clinical performance of the model. The statistical metrics are the coefficients of correlation between equal-time and lagged autocorrelations for the test dataset and digital twins of the validation dataset under the hypothesis that the correlations are equal between actual data and digital twins. Each autocorrelation contributes a weight to the coefficient of correlation proportional to the fraction of the test dataset present. That is, if $\mathbf{x}_t^{\text{data}}$ are covariates at visit t for the test dataset and $\mathbf{x}_t^{\text{twins}}$ are the same covariates for digital twins of subjects in the test dataset, then we compute the

Hyperparameter	Values
number of hidden units	$\lceil \frac{1}{2} n_{\text{vis}} \rceil$ (27), n_{vis} (53)
number of epochs	1250, 2500 , 5000, 10000
batch size	557 , 1113, 2226
initial learning rate	0.25 / n_{vis} , $0.5/n_{\text{vis}}$, $1/n_{\text{vis}}$
driven sampling σ_β	0, 0.15 , 0.3
ℓ_2 weight penalty	10^{-4} , 10^{-3}
adversary weight	0, 0.3 , 0.7
Monte Carlo steps (sampling)	100
optimizer	ADAM

TABLE III. The hyperparameter grid used to train the CRBM. The grid is defined as the Cartesian product of the values listed across hyperparameters. The value of each hyperparameter for the selected model is shown in bold. n_{vis} is the number of visible units. The batch sizes are defined so that there are 5, 10, or 20 batches per epoch in the combined training and validation datasets.

lag- ℓ autocorrelations,

$$C_\ell^{\text{data}} = \text{Cov}[\mathbf{x}_t^{\text{data}}, \mathbf{x}_{t+\ell}^{\text{data}}], \quad (\text{C1})$$

and equivalently for the digital twins. Taking $\mathbf{c}_\ell^{\text{data}}$ as a vector of unique non-trivial entries in C_ℓ^{data} multiplied by the fraction of data that was not missing in the calculation of the entries in C_ℓ^{data} , the metric is

$$R_\ell^2 = 1 - \frac{E[(\mathbf{c}_\ell^{\text{twins}} - \mathbf{c}_\ell^{\text{data}})^2]}{E[(\mathbf{c}_\ell^{\text{twins}} - E[\mathbf{c}_\ell^{\text{twins}}])^2]}. \quad (\text{C2})$$

These coefficients of correlation are computed for $\ell = 0, 1, 2, 3$ ($\ell = 0$ are the equal-time and $\ell > 0$ are the lagged autocorrelations).

The clinical metrics focus on the EDSS and relapse endpoints. All metrics are computed using 10 digital twins for each actual subject. They are:

- An absolute t -statistic for the CDW fraction in PPMS subjects. CDW is evaluated for each subject in the test dataset and their digital twins, \mathbf{w}^{data} and $\mathbf{w}^{\text{twins}}$, and the statistic is defined,

$$t_{\text{CDW}} = \frac{|E[\mathbf{w}^{\text{data}} - \mathbf{w}^{\text{twins}}]|}{\text{Var}[\mathbf{w}^{\text{data}}]^{1/2}} \sqrt{n}, \quad (\text{C3})$$

where n is the number of PPMS subjects for which CDW can be computed. We use 3 particular definitions of CDW, each of which defines chronic worsening as an increase of at least 1 point if the baseline EDSS is less than 6 and 0.5 otherwise, but vary in the required period of sustained worsening and duration over which it is measured (6-month sustained worsening over 1 year and 3-month and 6-month sustained worsening over 2 years). We define the metric as the average of z_{CDW} for these cases.

- An absolute t -statistic for the mean EDSS progression. The EDSS progression over 18 months is computed, \mathbf{s}^{data} and $\mathbf{s}^{\text{twins}}$, and a metric is defined,

$$t_{\text{EDSS}} = \frac{|E[\mathbf{s}^{\text{data}} - \mathbf{s}^{\text{twins}}]|}{\text{Var}[\mathbf{s}^{\text{data}}]^{1/2}} \sqrt{n}, \quad (\text{C4})$$

where n is the number of subjects for which the EDSS can be computed.

- The area under the receiver operating characteristic curve (AUC) that measures the model’s ability to predict relapses beyond baseline, through 18 months. The metric is the average AUC value for each visit from 3 to 18 months.

3. Model Selection

To identify the hyperparameters of the best performing model, the selection metrics were computed for each model successfully trained in the hyperparameter grid. We adopt a minimax approach to model selection, with the goal of selecting an optimal model that performs well for all metrics rather than optimizing performance on a single metric. Model selection comprises two steps:

1. For each metric, all N models are ranked from best performing (1) to worst performing (N). The maximum rank (worst performing) over all metrics of each model is recorded. The 25% of models with the lowest maximum rank are retained. This selects models that perform well across all metrics, rather than models that rank well for individual metrics and poorly in others.
2. For the surviving models, we re-rank the surviving models on each of the clinical metrics alone. The model that has the lowest maximum rank over these metrics is selected.

The combination of these two steps ensures we obtain models that perform well across all metrics and especially well on clinical metrics. The hyperparameters of the best performing model are shown in bold in Table III. These hyperparameters are used to train a model on the combination of the training and validation datasets.

Appendix D: Model Analysis

In this section we give quantitative details for the statistics shown in Figures 4, 5, and 6. We define $\mathbf{x}_t^{\text{data}}$ as the covariates at visit t for the test dataset and $\mathbf{x}_t^{\text{twins}}$ as the same covariates for digital twins of subjects in the test dataset.

In Figure 4 we compute several first and second order moments of test subjects and their digital twins. These statistics are, for $k = \text{data}$ and $k = \text{twins}$:

- Means for each covariate at each visit: $\mu_t^k = E[\mathbf{x}_t^k]$.
- Standard deviations for each covariate at each visit: $\sigma_t^k = \text{Var}[\mathbf{x}_t^k]^{1/2}$.
- Equal-time and lagged autocorrelations taken over all times, $C_\ell^k = \text{Cov}[\mathbf{x}_t^k, \mathbf{x}_{t+\ell}^k]$, for $\ell = 0, 1, 2, 3$.

All moments are computed over the subjects in the test dataset. For each statistic, we compute a regression between the values across covariates (or pairs of covariates) weighted by the fraction of data present for each particular point. For the correlations, this requires values for both covariates to be present for the statistic to be computed. For the means and standard deviations, because the values for different covariates can have very different scales, an ordinary least squares regression (and the corresponding coefficient of determination) is outlier sensitive, so we use Theil-Sen regression. For the correlations, ordinary least squares regression is sufficient, which allows us to report both the fit coefficients and the coefficient of determination.

In Figure 5, we compute a statistic that quantifies the observed covariate values for a given subject with the distributions predicted for that subject’s digital twins. As a start, for any covariate value for a single subject at a single visit we compute a p-value of the under the distribution of digital twins for that subject and visit:

$$p_{i,j,t}(x_i^{\text{data}}) = \Phi_{i,j,t}^{\text{twins}}(x_i^{\text{data}}), \tag{D1}$$

where $\Phi_{i,j,t}$ is the empirical cumulative distribution function of digital twins for covariate x_i of subject j at visit t . If the CRBM learns the exact distribution of the data, then the distribution of p-values should be uniform. One approach to testing statistical indistinguishability is to test the uniformity of this distribution using a 1-sample statistical test such as Kolmogorov-Smirnov. While quite powerful, it is challenging to interpret what a statistically significant result (a significant non-uniformity in the p-value distribution) means for the CRBM other than a failure to model the data distribution well. Instead, we focus on derived statistics that are much more interpretable.

From a p-value, we can compute a statistic from the inverse normal distribution,

$$\varphi_{i,j,t} = \Phi^{-1}(p_{i,j,t}). \quad (\text{D2})$$

These values should be normally distributed across subjects, and the moments are especially interpretable. If the mean is above (below) 0, then the mean of the model is lower (higher) than the mean of the data. If the variance is smaller (larger) than 1, then the variance of predictions of the model is larger (smaller) than the data. Note that the relationship between the moments and the bias of the model is inverted due to the fact that the statistic is comparing the data value to the model distribution. We plot the mean and standard deviation of these φ values in Figure 5. To test significance, we combine the mean and variance into a single statistic by computing a 1-sample Kolmogorov-Smirnov statistic between $\mathcal{N}(\text{E}[\varphi_{i,j,t}], \text{Var}[\varphi_{i,j,t}])$ and $\mathcal{N}(0, 1)$, using n samples for the former distribution. The significant level of the Kolmogorov-Smirnov test is adjusted by a Bonferroni correction on the number of test being performed, equal to the number of covariates evaluated (12) multiplied by the number of time points (12), for a scaling factor of 144 (meaning a comparison is significant if the p-value is less than $0.05/144$).

In Figure 6, we compare the complete set of longitudinal covariates between test subjects and their digital twins. We train a classifier model \mathcal{C} to predict whether given covariate values come from test subjects or their digital twins, and judge the performance of the classifier using the area under the receiver operating characteristic curve (AUC). An AUC score of 0.5 indicates that \mathcal{C} cannot do better than random chance at determining whether data comes from actual subjects or their digital twins, while an AUC of 1.0 indicates that \mathcal{C} can perfectly identify them. This is directly evaluating the statistical indistinguishability of digital twins.

The details of the comparison are as follows. Because different subjects can have different durations, we make comparisons at single visits or the difference between consecutive visits using all subjects still in their study at that visit (or pair of visits). Missing data is a potentially large source of bias in the comparison, since actual subjects have missing data while their digital twins do not. To correct for this, for each covariate we mean impute the missing data for actual subjects based upon the baseline values. For each subject, we assign the corresponding mean-imputed covariate values to their digital twins, meaning missingness or the imputed value cannot be used to differentiate subjects or their digital twins.

We make the comparisons using unregularized logistic regression for \mathcal{C} . The models are evaluated using 5-fold cross validation, and we repeat the evaluation for 100 trials, using a different digital twin of each subject for each trial. For each trial, we generate a digital twin for each subject and perform the mean imputation procedure described above, taking the relevant single visit or visit change data. We split the data into 5 mutually exclusive folds, each containing approximately 20% of the data. For each fold, we hold it out and combine the data from the 4 other folds and train a logistic regression model, evaluating the AUC on the held out fold. We average the AUC values over the 5 folds and report the result for the trial. The mean and standard deviation of these mean AUC values over trials is shown in Figure 6.